Modelling the lung in vitro

Riet, S. van

Chapter 3

Alveolus Lung-Chip cultures of patient-derived primary alveolar type-2 cells

Sander van Riet[1], Annemarie van Schadewijk[1], P. Padmini S.J. Khedoe[1], Jan J. Stolk[1], Pieter S. Hiemstra[1*], Anne M. van der Does[1*]

[1]Dept. of Pulmonology, Leiden University Medical Center, Leiden, the Netherlands

[*]Shared senior authorship

In revision at the American Journal of Physiology - Lung cell and molecular physiology

Abstract

Development of effective treatment strategies for lung tissue destruction as seen for example in emphysema would greatly benefit from representative human *in vitro* models of the alveolar compartment. Studying how (altered) biomechanical cues in emphysema affect alveolar epithelial repair function could provide new insight for tissue repair strategies. Preclinical models of the alveolus ideally combine human primary patient-derived alveolar type-2 cells (AEC2) with advanced cell culture applications such as breathing-related stretch, to more reliably represent the alveolar microenvironment. To test the feasibility of such a model, we isolated primary alveolar type-2 cells (AEC2) from patient-derived lung tissues including from severe emphysema, using magnetic bead-based selection of cells expressing the AEC2 marker HTII-280. We obtained pure alveolar feeder-free organoid cultures with use of a minimally modified commercial medium which also allowed for further expansion of these organoids. Following expansion, cells were seeded on Transwell PET inserts and on the Chip-S1 that has a flexible PDMS membrane enabling the application of dynamic stretch to cell cultures. AEC2 cultured for seven days on Transwells or the Alveolus Lung-Chip maintained expression of HTII-280, surfactant protein C (SP-C) and zonula occludens-1. When cultures were exposed to dynamic cyclic stretch for 5 days, cells remained viable, expressed HTII-280 and SP-C and displayed a slightly elongated organization. The combination of a straightforward culture method of patient-derived AEC2 and their application in Organs-on-Chips, enabling study of biomechanical cues in AEC2 functioning, provides a next step in the development of representative human preclinical models of the alveolar compartment.

Introduction

Chronic obstructive pulmonary disease (COPD) is one of the leading causes of death worldwide (World Health Organization 2018). Due to a lack of available curative treatments, combined with persistent and long-term effects of smoking, the alarming levels of air pollution as well as ageing of the population, this is not expected to improve in the near future (Khakban et al. 2017). Chronic airway inflammation and progressive destruction of the alveolar compartment of the lungs (emphysema) are principal hallmarks of this disease (Hogg and Timens 2009; Agusti and Hogg 2019). Alveolar tissue destruction reduces the gas exchange capacity and elastic recoil of the lungs, thereby progressively affecting quality of life of these patients. Smoking is one of the main risk factors for development of COPD. In addition to smoking cessation and pulmonary rehabilitation, pharmacological treatment for COPD is largely limited to the use of long-acting β2-agonists (LABA), long-acting muscarinic antagonists (LAMA) and inhaled corticosteroids, which do not modify the course of the disease (Miravitlles et al. 2016; Celli and Wedzicha 2019). Lung volume reduction surgery (LVRS) can give alleviation for patients as it improves breathing by resection of the most damaged part of the lungs.Otherwise, lung transplantation is the remaining treatment strategy when the decrease in lung function capacity becomes life threatening, but this is limited by the availability of matching donor lungs and rejection of transplanted lungs.

Development of new treatments that could halt or reverse the destruction of the alveolar compartment or potentially induce regeneration of lung tissue, are reliant on human preclinical models of the alveolar compartment, and available alternatives such as (tumour-derived) cell lines or animal models, unfortunately provide limited translation to *in vivo* human biology (Uhl and Warner 2015). Human induced pluripotent stem cells (hiPSC) offer an alternative source, however generation of AEC2 from hiPSC is currently still time consuming, costly and the derived alveolar cells generally display an immature phenotype (Jacob et al. 2017).

Isolation protocols of human AEC2 were until recently complex procedures that were generally time consuming, required specialized equipment and/or complex cell culture media (Witherden and Tetley 2001; Hiemstra, Tetley, and Janes 2019) and carried a risk of contamination with mesenchymal cells. Furthermore, when AEC2 are propagated in conventional *in vitro* cell culture they tend to differentiate over time to alveolar epithelial type-1 cells (AEC1)

(Mao et al. 2015). Finally, since culture-based expansion of AEC2, and therefore the yield of AEC2 is limited, the number of isolated cells restricts the experimental set-up. Recently, new methods have been published that overcome many of these limitations, demonstrating the isolation of murine or human AEC2 from lung tissue and subsequent expansion in organoid culture (Glisinski et al. 2020; Salahudeen et al. 2020; Katsura et al. 2020). These much needed improvements have already shown to be a great step forward, and a logical next step is to apply primary AEC2, preferably patient-derived, in preclinical models of the alveolar compartment that include additional aspects of the alveolar environment, such as capillary blood flow and strain caused by breathing motions, as these mechanical forces are highly relevant in the alveolus environment but currently understudied (Evans and Lee 2020). The development of Organs-on-Chips that recapitulate the tissue architecture more closely and allow integration of the dynamic biomechanical changes and cellular interactions within tissues is highly needed (Benam et al. 2016; Zamprogno et al. 2021).

To provide proof-of-principle for a cell culture model that more reliably mimics the alveolus microenvironment, we used a straightforward two-step protocol for AEC2 isolation from resected human lung tissue derived from non-smokers, ex-smokers, smokers and emphysematous tissue from lung volume reduction surgery (LVRS) surgery. Dissociation of the lung tissue was followed by an HTII-280-based enrichment step of AEC2 using magnetic beads, recently also developed by Katsura and colleagues (Katsura et al. 2020). This isolation procedure was combined with a feeder-free organoid-based culture method that allows expansion and propagation of AEC2 for weeks up to several months, whilst maintaining AEC2 characteristics and preventing contamination by other cells using a minimally modified commercial medium. Once sufficiently expanded, cells were used for successful culture on conventional Transwells and innovative Organs-on-Chips, in which we demonstrated feasibility of using the organoid-expanded AEC2 to study the effect of cyclic stretch on AEC2 phenotype.

Methods

Isolation, maintenance and expansion of primary alveolar type-2 cells

Tissue processing: Alveolar type-2 cells (AEC2) were isolated from tumour-free tissue from patients undergoing lung resection surgery for lung cancer (smokers, ex-smokers and non-smokers) or from emphysematous tissue from patients undergoing LVRS at the Leiden University Medical Center (LUMC, The Netherlands) for emphysema. Patient characteristics are summarized in Table 1. The use of surplus lung tissue for research following surgery was within the framework of patient care and in line with the "Human Tissue and Medical Research: Code of conduct for responsible use" (2011) (www.federa.org) and followed advice of the LUMC Medical Ethical Committee. Tissue donation was based on a no-objection system for coded anonymous use of waste tissue, left-over from diagnostic or therapeutic procedures. "No-objection" negates the need for individual informed consent. All methods were carried out in accordance with relevant guidelines and regulations.

	Lobectomy	**LVRS**
Number of donors	17	14
Male/Female	12/5	4/10
Age (years) mean [SD]	62.3 [11.3]	57.1 [2.3]
BMI mean [SD]	27.1 [6.3]	23.3 [2.1]
Smoking Status (non-/ex-/smokers)	3/5/6#	0/14/0
Pack years (ex-/smokers) [SD]	22.8 [15.8]/42.40 [9.56] ##	18.4 [3.4]/-
FEV1 % pred [SD]	89.40 [19.43]###	30.1 [7.7]
DLCO % pred [SD]	79.50 [24.58]#	38.1 [11.4]

Table 1. Patient characteristics of resected lung tissue from lobectomy surgery or lung volume reduction surgery (LVRS). Abbreviations: SD (standard deviation); BMI (body mass index); FEV1 (forced expired volume in 1 sec); DLCO (diffusion capacity of the lungs for carbon monoxide)

#Data available from 14 lobectomy patients

Smokers data available from 5/6 lobectomy patients

Data available from 15 lobectomy patients

The lung tissue homogenate preparation procedure was adapted from Witherden et al. (Witherden and Tetley 2001).Resected lung tissue was cut into pieces of approximately 5 cm^3 and injected with 7.5 mL trypsin (Gibco 1:250) (0.25% w/v) in Hanks' Balanced Salt Solution (HBSS)) (ThermoFisher, Waltham, MA) and incubated for 15 min at 37°C; this wasrepeated for a total incubation time of 45 min. Trypsin activity was inhibited by

injecting the tissue with 7.5 mL soybean trypsin inhibitor (SBTI; 0.1% w/v in HBSS; St. Louis, Sigma-Aldrich, MO). Next, tissue was manually cut to as small as possible pieces during max 10 min. at room temperature (RT). The processed tissue was collected in gentleMACS C tubes (Miltenyi, Leiden, Netherlands) and ran twice on the gentleMACS tissue dissociator program M_lung_02.01 (Miltenyi) for further processing. This solution was then passed through a metal sieve to remove the biggest remaining pieces of tissue and next through a strainer with a mesh size of 100 μm (VWR international, Amsterdam, Netherlands) to obtain a single cell suspension. The cells were centrifuged for 5 min at 265 × g and supernatant was removed. If necessary (donor dependent), a red blood cell lysis (Miltenyi) was performed. To this end, the cell pellet was resuspended in 1 mL magnetic-activated cell sorting (MACS) buffer consisting of PBS, 0.1% (w/v) BSA (Sigma-Aldrich) and 2 mM EDTA (ThermoFisher) to continue with HTII-280$^+$ selection.

HTII-280$^+$ selection: HTII-280$^+$ AEC2 were isolated using a HTII-280 monoclonal mouse IgM antibody (Terrace Biotech, San Francisco, CA). Total tissue homogenate in 1 mL of MACS buffer was incubated with 25 μL of undiluted HTII-280 antibody for 15 min at 4°C. Following 5 min. centrifugation at 265 × g, cells were incubated with magnetic bead-labelled anti-mouse IgM (Miltenyi) for 15 min at 4°C and subsequently MACS selection was performed according to manufacturer's instruction (Miltenyi).

Culture of alveolar type-2 cells in organoids: HTII-280$^+$ cells were collected by centrifugation at 265 × g for 5 min AEC2 were counted in trypan blue and resuspended in cold Basement Membrane Extract 2 (BME2, Cultrex, Gaithersburg, MD). Alveolar cells (1*10^5 viable cells/30 μL droplet/well) were seeded in a 48 well plate, after which droplets were allowed to solidify at 37°C. After 10 min, 500 μL complete alveolar organoid medium was added to the well. Alveolar cell culture medium consists of alveolar medium (Sciencell, Carlsbad, CA) with all supplements from the media kit except the antibiotics, which were replaced by the addition of Primocin (Invivogen, San Diego, CA). Alveolar cell culture medium supplemented with 4 μM CHIR99021 (CHIR; Sigma-Aldrich) is further referred to as "complete alveolar organoid medium". At the start of culture or directly upon passaging (until next medium refreshment), the complete alveolar organoid medium was supplemented with 10 μM Y-27632 (Cayman Chemical, Ann Arbor, MI) for 48 h. Medium was refreshed twice a week and cells were passaged approximately every 2 weeks adapting the passing time to the specific donor growth-rate.

For passaging, medium was aspirated, and cold PBS was added to the well to dissolve the BME2. The organoid suspension was collected and incubated for max 10 min using 1 mL 0.03% w/v trypsin (1:250; Gibco, ThermoFisher), 0.01% (w/v) EDTA (BDH, Poole, England), 0.1% glucose (BDH) in PBS per droplet at 37°C. Two mL SoyBean Trypsin Inhibitor (SBTI; Sigma) solution per droplet was added to stop the trypsin activity and organoids were further dissociated into fragments by resuspension. The disrupted organoids were centrifuged, resuspended in BME2 and re-plated. Organoids were subsequently grown under standard cell culture conditions (37°C and 5% CO2).

Cytospin preparations: To validate the success of HTII-280$^+$ isolation using magnetic beads, cytospin preparations were obtained from the lung tissue homogenate single cell suspension before selection (unsorted) and after HTII-280$^+$ selection, also including the negative fraction (flow through). Cytospin preparations were fixed using 4% formaldehyde (Sigma Aldrich) in PBS for subsequent immunofluorescence staining.

Transwell cultures: Transwells were coated with a mixture of 30 μg/mL bovine collagen I (PureCol; Advanced BioMatrix, San Diego, CA), 10 μg/mL BSA (ThermoFisher), and 10 μg/mL fibronectin (Promocell, PromoKine, Bio-connect, Huissen, The Netherlands) in PBS and seeded with either the HTII-280$^+$ lung cells directly isolated from tissue (P0) or with the dissociated alveolar cells from the organoids at various passages. Alveolar medium was added to the basal and apical compartment of the Transwells and refreshed twice a week. After 7 days in culture, the Transwells were fixed for immunofluorescence staining using 4% formaldehyde in PBS.

Alveolus Lung-Chip cultures: Both channels of the commercial Chip-S1 (Emulate Inc, Boston, MA) were activated using the provided reagents ER-1 and ER-2. In short, ER-1 was resuspended in 5 mL ER-2 buffer and directly pipetted into both channels of the chip. Next, the chips were placed under UV-light for 10 min followed by two washes of both channels with ER-2, followed by another round of ER-1, UV and ER-2 washes. After the second ER-2 wash, the channels were washed with PBS. Next, both channels were filled with 300 μg/mL human collagen IV (Sigma-Aldrich) solution in PBS, and incubated overnight at 37°C and 5% CO2, to allow deposition of the collagen on the membrane in the Chip-S1.

Next, both channels were washed with complete alveolar organoid medium before cells were seeded in the top channel. To seed sufficient AEC2, 9 x 30 μl

organoid-containing drops of alveolar cells were collected per chip, and organoids were dissociated as described when passaging the organoids. The cell pellet was resuspended in complete alveolar organoid medium and 30 µL of this cell suspension was used to seed the top channel of one chip. Cells were left to adhere for approximately 6 h in the incubator in presence of 10 µM Y-27632. Next, top and bottom channels were infused with pre-warmed complete alveolar organoid medium containing 10 µM Y-27632, and Chips were connected to pre-warmed media-filled fluidic manifolds, named Pods (Emulate Inc.). After obtaining liquid-liquid interface connection between Chips and Pods, these units were placed in the micro perfusion instrument, named "Zoë" (Emulate Inc.). After finishing the initial regulate cycle program (which pressurizes the medium to increase gas solubility and removes nucleating air bubbles while the system calibrates), the Alveolus Lung-Chips were continuously perfused at a flow rate of 30 µL/h in both the top and bottom channel. Approximately 24 h after this first regulate cycle program, a so-called via-wash was performed, dislodging any bubbles in the Pod's reservoirs fluid vials, followed by a second regulate cycle. Alveolar medium in the Pods was refreshed after 48 h (no addition of Y-27632), which was repeated every other day throughout the time of culture (all without Y-27632). When the cultures reached confluence (usually between ~2-4 days post-seeding), chips were divided into two groups: control (flow rate 30 µL/h top and bottom channel flow conditions) and stretch (30 µL/h top and bottom channel flow conditions + 10% stretch at 0.25Hz) (Huh et al. 2010).

Imaging of cytospin preparations, organoids, Transwells and Chips

Cytospins preparations and Transwells: Fluorescent staining was performed on cytospin preparations, cells cultured on Transwells, and paraffin sections of the organoids according to the following protocol. In brief, after fixation cells were incubated with permeabilization and blocking buffer (1% w/v BSA, 0.3% v/v Triton-X100 (Sigma-Aldrich) in PBS) for 30 min at 4°C. Paraffin sections were pre-treated with DAKO pH 9 antigen retrieval solution according to manufacturer's instruction (DakoCytomation, Denmark, Glostrup). The primary antibody (Table 2) was added in blocking solution to the cells for 1 h at RT. Next the samples were washed with PBS and incubated with fluorescent-labelled secondary antibody together with 4′,6-Diamidino-2-phenylindole (DAPI; Sigma-Aldrich) for 30 min at RT.

Organoids: After dissolving the droplets with recovery solution (Corning,

Corning, NY), the alveolar organoids were fixed in 4% formaldehyde (FA) in PBS for 30 min. Next the organoids were taken up in 2% (w/v) low melting agarose (ThermoFisher) and embedded in paraffin. Slices of 4 µm were cut and the organoids were stained with various antibodies or H&E staining. All antibodies used can be found in Table 2.

Alveolus Lung-Chips: Alveolar cells in the chips were washed with PBS and fixed using 4% PFA solution, which was pipetted into both channels and incubated for 20 min at RT, washed with PBS and stored in PBS at 4°C until staining. Chips were subsequently removed from the carrier and cells were blocked and permeabilized using 0.5% (v/v) Triton-X 100 in PBS with 5% BSA for 1 h at RT. Chips were cut into 2 pieces using a razor blade and channels were filled with primary antibodies (Table 2) diluted in the Triton/BSA buffer and incubated for 1 h at RT. Samples were rinsed three times for 5 min with PBS. Next, channels were filled with secondary antibodies diluted in Triton/BSA buffer which was left incubating for 1 h at RT, followed by a triple 5 min wash with PBS. DAPI was used to stain cell nuclei. Channels were next filled with prolong gold anti-fade (Thermo Scientific) and stored in the dark at 4 °C until imaging. Chips were imaged on coverslips 25x75mm (Bellco Glass, Vineland, NJ, U.S.A via Electron Microscopy Sciences, Hatfield, PA) with 0.13-0.17 mm thickness using a Leica DMi8 microscope equipped with an Andor Dragonfly 200 spinning disk confocal using a 10x objective (NA 0.30), 20x water objective (NA 0.50) or 40x water objective (NA 0.80).

Primary Antibody	Species	Company	Cat. No.	Dilution
HTII-280	Mouse	Terrace Biotech	TB-27AHT-280	1:200
HTI-56	Mouse	Terrace Biotech	TB-29AHT1-56	1:50
Surfactant protein C	Rabbit	EMD Millipore	Ab3786	1:100
E-cadherin	Mouse	BD Transduction Laboratories	610182	1:400
RAGE	Rabbit	R&D systems	AF1145-sp	1:50
Keratin 5	Rabbit	Abcam	ab52635	1:200
ZO-1	Mouse	ThermoFisher	339100	1:100

Secondary Antibody	Company	Cat. No.	Dilution
Alexa Fluor 448 Donkey anti Mouse	ThermoFisher	A21202	1:200
Alexa Fluor 568 Donkey anti Mouse	ThermoFisher	A10037	1:200
Alexa Fluor 448 Goat anti Rabbit	ThermoFisher	A11008	1:200
Alexa Fluor 568 Donkey anti Rabbit	ThermoFisher	A10047	1:200

Table 2. Antibodies

Results

Generation of alveolar type-2 organoid cultures from homogenized lung tissue

We developed a straightforward procedure for isolation of AEC2 from human lung tissue, that was recently also reported by another group using healthy tissue (Katsura et al. 2020). We dissociated macroscopically normal lung tissue derived from lung cancer patients with or without a smoking history (current smokers, ex-smokers and non-smokers) and additionally, for the first time to our knowledge, also used emphysematous lung tissue from LVRS surgery and obtained a single cell suspension using protease digestion. We subsequently cultured this single cell suspension in BME2 droplets. AEC2 organoid formation was rarely observed unless the commercial alveolar medium was supplemented with the canonical WNT activator CHIR99021 (CHIR; a GSK3 inhibitor), resulting in formation of predominantly alveolar organoids in P0 and pure cultures after the first passage (Fig. 1A&B). To confirm that the use of specialized media was sufficient to direct AEC2 organoid formation from the total lung homogenate suspension, we next cultured the total lung homogenate suspension in our complete alveolar organoid medium or in specialized airway organoid medium (Sachs et al. 2019). When cells from the homogenate were cultured in complete alveolar organoid medium, organoids generated were characterized by presence of the alveolar marker HTII-280 and absence of the airway basal cell marker keratin 5 (HTII-280^{+}/KRT5^{-}). Using the airway organoid medium, the development of predominantly bronchial organoids was observed (HTII-280-/KRT5^{+}; Fig. 1C&D). Although HTII-280^{+}-cell clumps were visible in these cultures, they remained small and did not progress into organoid development. However, despite developing a successful medium to support alveolar organoid formation, we noticed that some isolations failed. Characterization of the HTII-280^{+} population in the lung homogenate suspension using cytospin preparations, showed a strong donor-dependent ratio of AEC2 to other cells. We therefore hypothesized that as a result, the AEC2 to other cell ratio per gel drop was insufficient in some donors for successful establishment of alveolar organoids. To overcome this issue, we decided to include an enrichment step for AEC2.

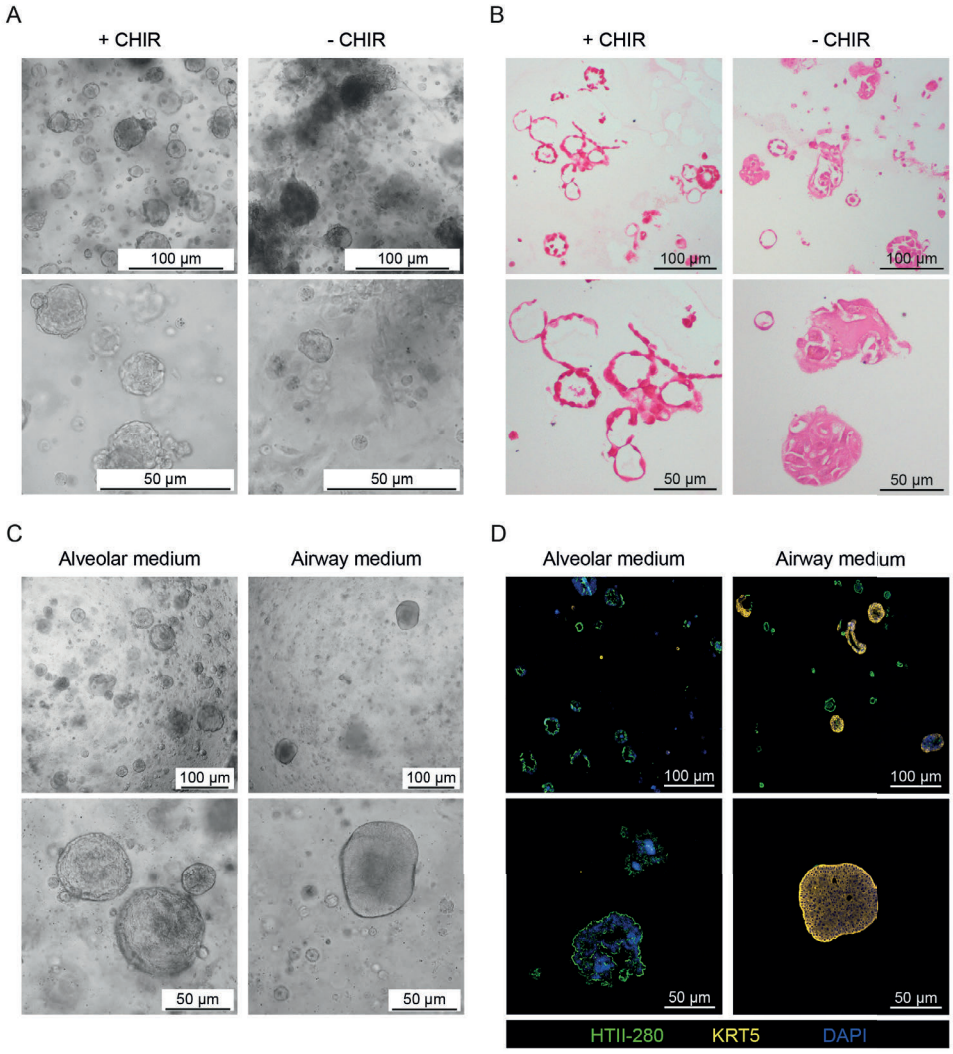

Figure 1. Generation of alveolar type-2 organoid cultures from homogenized lung tissue. Lung tissue was enzymatically digested to obtain a single cell suspension which was subsequently cultured in BME2 drops. A, Brightfield imaging of organoids cultured in alveolar medium supplemented with (+) or without (-) 4 µM CHIR, a GSK3 inhibitor. B, Brightfield images of H&E staining of AEC2 cells cultured in alveolar medium supplemented with (+) or without (-) CHIR. Representative images of experiments performed with N=3 different donors (A, B). C, Brightfield images of organoids cultured from lung tissue homogenate in alveolar medium (including CHIR) or airway organoid medium. Representative image of experiments performed with N=3 different donors. D, Fluorescent imaging of organoids stained for HTII-280 (AEC2, green) and Keratin 5 (KRT5; airway basal cells, yellow), nuclei were stained with DAPI (blue).

Alveolar type-2 cell enrichment from peripheral lung tissue homogenate by HTII-280⁺ selection

Our initial studies revealed that cell cultures started from the whole lung homogenate caused issues with obtaining sufficient AEC2 for organoid

formation in some donors. Therefore, an enrichment step was included to first isolate AEC2 from the lung tissue homogenate. Isolation of AEC2 from peripheral tissue either by selection via adherence steps or EpCAM^{+} epithelial cell sorting results in an undesired mixture of cell types, including AEC2 but also airway epithelial cells and mesenchymal cells. A decade ago, Gonzalez and colleagues showed that the AEC2 marker HTII-280 could be

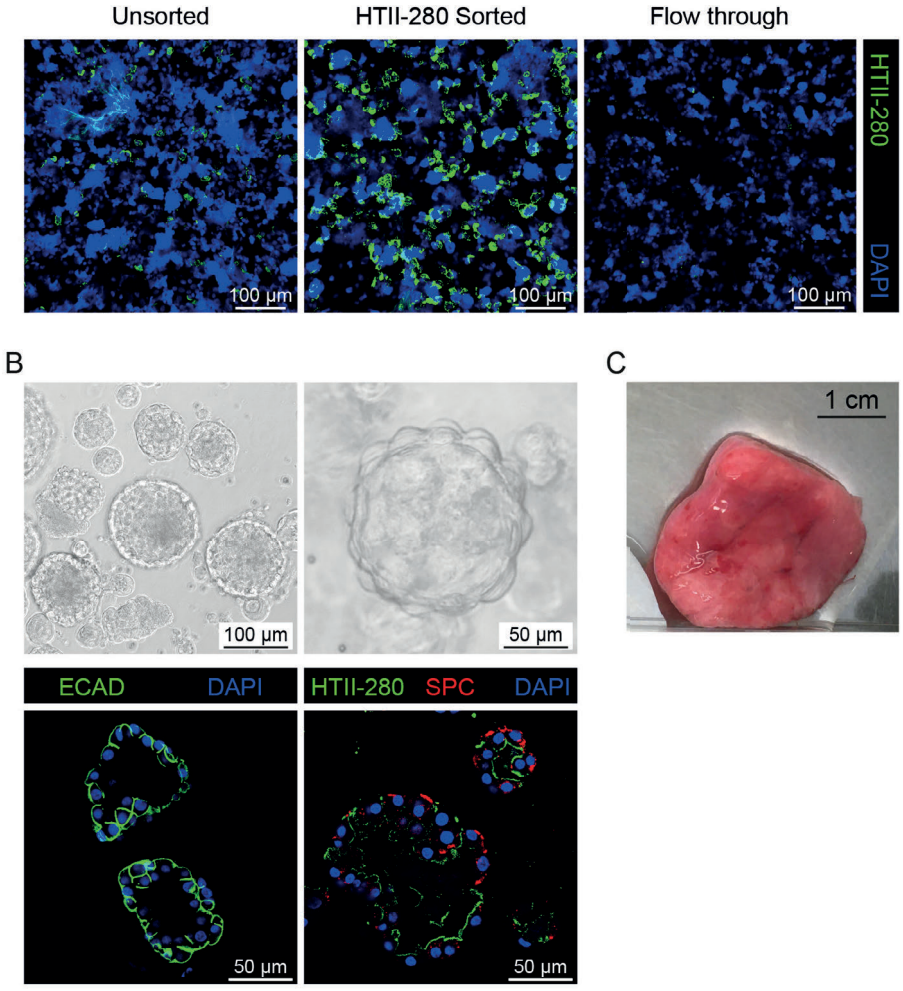

Figure 2. HTII-280^{+} selection of alveolar type-2 cells from homogenized lung tissue. Lung tissue was enzymatically digested to obtain a single cell suspension, after which HTII-280 selection via magnetic beads was performed. Sorted cells were subsequently cultured in BME2 drops. A, Representative immunofluorescent images of cytospin preparation of lung tissue homogenate (unsorted, sorted and the flow-through after sorting). AEC2 were stained with HTII-280 (green) and DAPI (blue) for nuclei staining. Representative image from N=3 independent experiments with different donors. B, Representative brightfield images of organoids derived from the HTII-280^{+} fraction cultured in alveolar medium. Representative image from N=4 independent experiments with different donors. Fluorescent images of organoids stained for HTII-280 (AEC2, green) and surfactant protein C (SP-C, red); nuclei were stained with DAPI (blue). Representative images of N=4 different donors. C, Example of amount of lung tissue that is minimally required to isolate sufficient cells for AEC2 organoid development.

used to increase the purity of the AEC2 population (Gonzalez et al. 2010). This method was based on fluorescence-activated cell sorting (FACS), which requires expensive equipment, skilled personnel and is time-consuming. Here we decided to integrate a magnetic bead-based isolation, that was recently also reported by Katsura at al. (Katsura et al. 2020). Lung tissue homogenate was incubated with an HTII-280 antibody, and next coupled to anti-mouse IgM-coated magnetic beads to allow magnetic bead-based AEC2 isolation. Although 100% pure AEC2 populations could not be achieved using this method, the enrichment was significant (Fig. 2A). Using this method, in combination with our complete alveolar organoid medium, we could obtain sufficient AEC2 to establish successful organoid cultures (Fig. 2B), while needing only relatively small pieces of tissue (Fig. 2C). We obtained a >85% (N=8/9 isolations) success rate using the finalized method for the formation of alveolar organoids up to P1. This method of isolation proved successful when using peripheral tissue obtained from macroscopically normal lung tissue from lung cancer surgery with or without a smoking history or COPD. In addition, AEC2 isolation from emphysematous lung tissue removed during LVRS for severe emphysema was successful in ~71% (10/14) of isolations, using different versions of the protocol, but successfully validated with the final protocol presented in the methods section for one donor.

Propagation and expansion of primary alveolar type-2 cells in feeder-free organoid cultures

After AEC2 enrichment by HTII-280^{+} selection, the cells were cultured in BME2 to allow organoid formation with the aim to propagate and expand the AEC2 for future experiments. We cultured the isolated AEC2 in a feeder-free

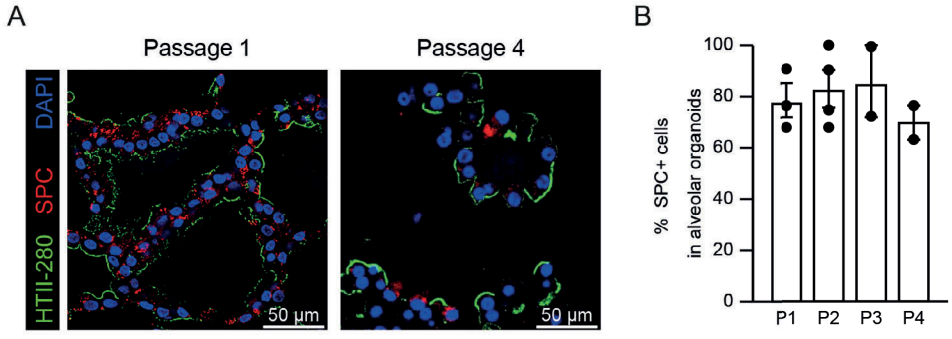

Figure 3. Propagation and expansion of primary alveolar type-2 cells AEC2 *in vitro*. A, Representative immunofluorescent images of a cross-section of embedded AEC2 organoids after passage 1 and after passage 4. Cells are stained for HTII-280 (green) and surfactant protein C (SP-C, red) and nuclei with DAPI (blue). B, Quantification of SP-C^{+} cells in organoids cultured at different passages (P#). N=2-4 different donors.

organoid system and were able to propagate the AEC2 organoids for weeks to months, depending on the donor, while maintaining AEC2 characteristics and increasing cell numbers (Fig. 3A). Generally, AEC2 were used for experiments before cessation of growth, but when propagated, P6 could be reached. It remains unclear which factor(s) play(s) a role in cessation of organoid growth. On average 80% of cultures that reached P1 were also able to reach passage P3. HTII-280 expression remained positive for all cells in the organoids over time of passaging (Fig. 3A) as well as surfactant protein C (SP-C) expression (Fig 3B), although SP-C decreased in organoids from some donors. Interestingly, propagation and expansion rates were similar between macroscopically normal lung tissue and LVRS-tissue derived AEC2 (observation), even though LVRS-resected lung tissue constitutes the most damaged part of the emphysematous lung.

Culturing alveolar type-2 cells on Transwell and Alveolus Lung-Chip cell culture platforms

To validate that patient-derived AEC2 propagated as organoids were suitable for experiments on traditional Transwells and an Organs-on-Chips platform, we dissociated the alveolar organoids and seeded them on Transwell or Lung-Chips. For Transwell we used a collagen I/fibronectin/BSA coating, since collagen IV coating did not result in successful attachment of the cells to the Transwell PET membrane. In contrast, for the Alveolus Lung-Chip, collagen IV coating resulted in a good attachment of the cells. AEC2 were kept in submerged culture for 7 days after which we fixed the cells and stained for AEC1 and AEC2 phenotypic markers and tight junctions. We found that AEC2 cultured for seven days, maintained expression of type-2 markers HTII-280^{+} and/or SP-C^{+}, and ZO-1 staining throughout the monolayer (Fig. 4A), whereas AEC1 markers HTI-56 and RAGE could not be detected.

Since Organs-on-Chips technology allows a closer representation of the *in vivo* lung microenvironment compared to Transwells, we were interested in investigating how breathing-like motions such as cyclic stretch may preserve primary AEC2 phenotype in culture. To investigate this, we seeded the Alveolus Lung-Chip with AEC2 from 1 to max. 6 donors (donor mix) that were expanded via organoid culture and allowed the cells to reach confluency in 2-3 days. Next, we cultured the cells for an additional 5 days submerged in the presence or absence of dynamic stretch. We noticed a quick but small change in morphology of the cells cultured in the chips

that were exposed to dynamic stretch, which was more pronounced in some donor mixes than others (Fig. 4B). Next, we assessed HTII-280 and SP-C expression after 5 days of submerged culture in presence or absence of dynamic stretch. AEC2 are known to spontaneously differentiate toward an AEC1 phenotype in culture (Zhao, Yee, and O'Reilly 2013) , but after 5 days we still found a substantial amount of HTII-280^{+} cells in both the control

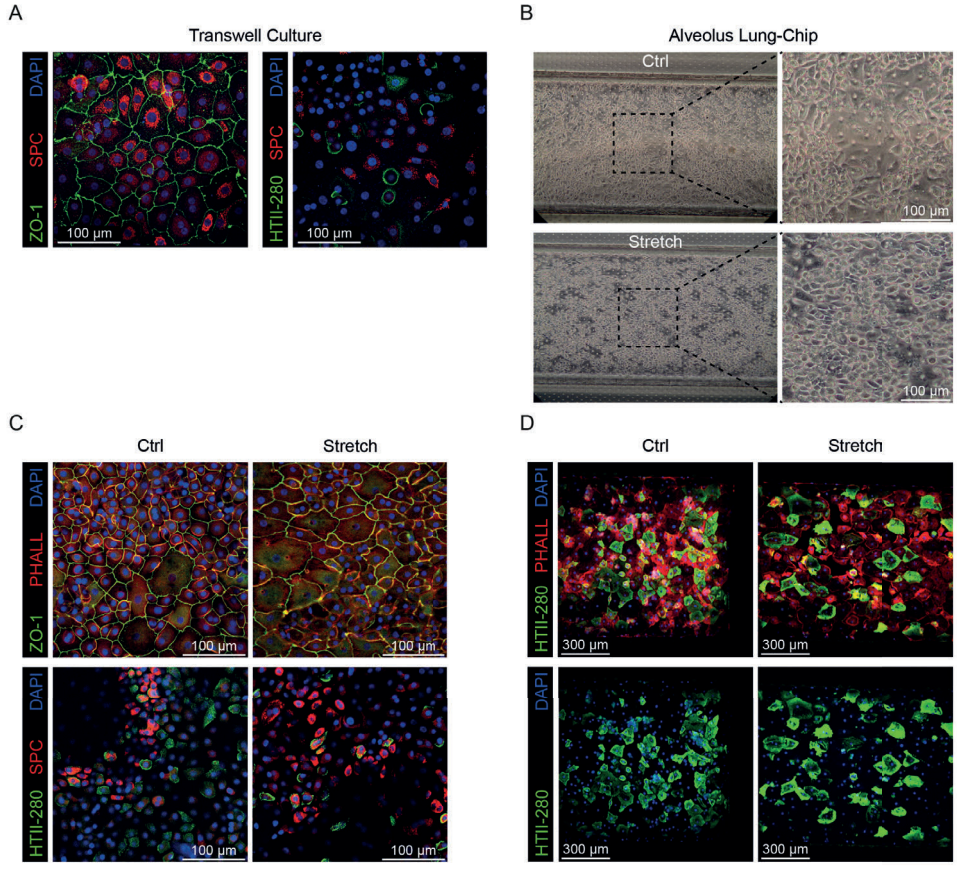

Figure 4. Alveolar type-2 cell culture after expansion as organoid on the Transwell and Alveolus Lung-Chip platform. Organoids from donors at different passages were dissociated, mixed and seeded on Transwells or the Alveolus Lung-Chip for seven days. A, Fluorescent images of Transwell cultures of AEC2 after seven days of culture. Cells were fixed and stained for HTII-280 (green), surfactant protein C (SP-C, red) or ZO-1 (green) and nuclei with DAPI (blue). Representative image from N=4 independent experiments with different donor(mixes). B, Representative images of Alveolus Lung-Chip: AEC2 organoids were dissociated and seeded on the Alveolus Lung-Chip platform and cultured for 5 days after reaching confluency (generally within 2-3 days). During these 5 days, some chips were exposed to 10% dynamic stretch at 0.25Hz (stretch). C, Cells in the chips were fixed and cut into two parts, ZO-1 (green), phalloidin (red) and a nuclei stain (DAPI, blue) were combined in one half of the chips, in the other half, AEC2 were stained with HTII-280 (green) and surfactant protein C (SP-C, red) and nuclei using DAPI (blue). N=4 independent experiments using different donor (mixes) per experiment, 1 chip each. D, Fluorescent images of Alveolus Lung-Chip cultures that were seeded with a lower cell density as the chips cultured in B, displaying different morphology with larger cell size. Cells were stained with HTII-280 (green) and surfactant protein C (SP-C, red) and nuclei using DAPI (blue).

and stretch-exposed chips and ZO-1 expression throughout (Fig. 4C). Since we were not successful in counting the cells in the dissociated organoid suspension, as we do not obtain a completely single cells suspension, we had variable seeding densities between experiments and we did observe that in some experiments the initial seeding density was lower than anticipated, but despite this the cells reached confluence and expressed HTII-280 (Fig. 4D). However, when these cells underwent dynamic stretch, some areas showed signs of cell detachment, suggesting that under these additional forces the cells may experience difficulties staying attached to the membrane when initial cell number is rather low. In addition, these cells displayed a different morphology as they were larger in size (Fig. 4D).

Discussion

Here we present a proof-of-principle application of AEC2 isolated from relatively small pieces of patient-derived emphysematous and non-emphysematous lung tissue, which after feeder-free expansion could be cultured on classical Transwell and the Alveolus Lung-Chip. AEC2 isolation was successful in relatively healthy unaffected lung tissue but also in tissue from long-term smokers, COPD patients and emphysematous lung tissue that was removed during lung volume reduction surgery. Strikingly, even this emphysematous tissue yielded high numbers of AEC2, demonstrating the versatility of this protocol for use with both healthy and (very) diseased lung tissue. Using a straightforward isolation and expansion method, we could culture these AEC2 for weeks up to months in organoids while maintaining AEC2 marker expression (Lamers et al. 2021). When expanding AEC2 using conventional 2D culture, the transient loss of AEC2 phenotype and the increase in AEC1 makers restricts studies from being performed over longer time periods and also limits the comparability between independent experiments. Using our newly developed protocol we observed that after 7 days of culture on the Alveolus Lung-Chip, HTII-280^{+} and/or SP-C$_{+}$ cells were still present, which provides future possibilities to perform functional assays on regenerative potential of AEC2.

The usefulness of HTII-280 as a marker for the isolation of AEC2 has been demonstrated previously (Glisinski et al. 2020; Gonzalez et al. 2010; Katsura et al. 2020). Isolation of AEC2 based on HTII-280 proved successful as the enrichment step was found to be essential due to the variable proportions of AEC2 in the total isolated cell suspension derived from different tissues.

Although we obtained a pure alveolar organoid culture upon passaging of the organoids, we did find additional non-epithelial cells in the isolated population at the initiation of organoid culture (P0). However, these cells were no longer present in our culture after the first passage. There was almost no contamination with airway epithelial cells in the alveolar organoid cultures after the first passage.

When we cultured the cells from the whole lung tissue homogenate (all epithelial cells still present) in airway organoid medium (Sachs et al. 2019), we obtained predominantly $KRT5^+$ airway organoids and many small alveolar cell clumps that did not develop further. Conversely, when the lung homogenate was cultured in complete alveolar organoid medium, analysis of the culture revealed little to no $KRT5^+$ airway epithelial cells but predominantly HTII-280$^+$ AEC2 organoids. Although these observations provide strong support for the selection pressure issued by these specialized media, we cannot exclude that the non-AEC2 present after isolation and during the start of the culture may influence success of the alveolar cell cultures during the first or succeeding passages. Therefore, if required, for example when cells are directly used in experiments, the purity of the AEC2 population after isolation could be further optimized. To this end, we have so far also tested depletion of leukocytes via CD45 selection, which did not affect organoid formation. If sufficient AEC2 are present in relation to the other cells in the homogenate, this application however does allow for culture of small airway epithelial organoids and alveolar organoids from the same donor, with cells derived from adult tissue.

AEC2 are notoriously difficult to cryopreserve and this issue has unfortunately not been resolved yet but is focus of our current activities. Nevertheless, we were able to store pieces of unprocessed resected lung tissue at -80°C for longer periods of time (weeks) and still successfully isolated AEC2, although isolation of AEC2 from fresh tissue was preferred as this resulted in a significant better yield.

We observed that whereas alveolar cells grown in organoids retained HTII-280 expression, some of the organoid cultures (donor dependent) were found to decrease expression of SP-C upon prolonged culture. This raises the question of which additional markers should be used to define AEC2. The loss of SP-C was previously interpreted as a loss of AEC2 phenotype (Zhao, Yee, and O'Reilly 2013; Mao et al. 2015), however also AEC2 cultured on Transwell and chip demonstrated both HTII-280 and SP-C double or

single-positive cells. Transcriptomic analysis has revealed various subsets of alveolar cells, characterized by expression of subset-specific genes (Choi et al. 2020). These markers could potentially be interesting to use in the cultures used in this study. In addition, Choi and co-workers additionally showed that various alveolar cell subsets could be derived from AEC2 by exposure to (macrophage-derived) IL-1β in mice. It would be interesting to assess whether this approach also affects human AEC2 differentiation in culture. Interestingly when isolating AEC2 from LVRS donors, we did not observe a difference in growth rate or organoid number, suggesting that these properties are not affected by in cells isolated from an emphysematous environment. One explanation could be is that the isolation procedure selects for a more robust AEC2 subset from this tissue, that may be present in varying amount in tissue from different donors. However, although tissue pieces from different donors are difficult to compare, we did not experience that yield was lower from LVRS tissue compared to the other tissues. Alternatively, differentiation from AEC2 to AEC1 may be impaired or affected in LVRS tissue, and therefore it will be interesting to further study this and other characteristics of these cells in culture.

When seeding the dissociated AEC2 organoids on Transwell or Alveolus Lung-Chip, we could still detect HTII-280 expression and/or SP-C after 7 days of culture. We tried to determine AEC1 numbers after these 7 days of culture, however expression of established markers for AEC1 (Kobayashi et al. 2020), HTI-56 and RAGE, could not be detected. It is unclear whether this relates to a technical issue or whether we were unable to achieve AEC1 differentiation by using our complete alveolar organoid medium. Investigations are ongoing to gain insight into this observation, but we speculate that the supplementation of CHIR contributes to the lack of observed AEC1 markers. The effect of canonical WNT activation on the propagation and AEC2 morphology has been described previously in organoid cultures (Nabhan et al. 2018).

The magnetic bead-based solution for enrichment of the AEC2 population in the lung homogenate suspension described here and previously (Katsura et al. 2020) greatly improves the workflow and time for AEC2 isolation, and also the use of minimally modified commercial medium limits the high costs often associated with feeder-free organoid culture. Being able to dissociate the expanded organoid cultures for seeding on Transwell and/or Lung-Chips allows a large range of experimental set-ups including those with gaseous exposures, or application of viruses on the luminal side of the alveolar cell

cultures once air-liquid interface cultures have also been validated with use of this procedure. Successful isolation from diseased tissue also extends the possible experimental approaches significantly and allows to study repair and regeneration using cells derived from a relevant microenvironment. A limitation of the method presented here as well as those of others, is that the rate of proliferation of the AEC2 is relatively low and the time it takes to obtain sufficient cells for experiments also depends on the initial yield of AEC2. In Alveolus Lung-Chip cultures, for example, the number of cells needed is still significant, which limited our experimental set-up and necessitates the use of donor mixes instead of single donors for use in experiments. Future endeavours will aim to promote expansion by modulation of signalling pathways, and use of AEC2-AEC1 differentiation media (Katsura et al. 2020) by determining those culture conditions that allow control over AEC2 to AEC1 differentiation, possibly by further modulation of WNT signalling (Zacharias et al. 2018).

The unique set-up of the Alveolus Lung-Chip allows for the implementation of cyclic stretch on the alveolar cell cultures (Hassell et al. 2017; Huh 2015). Especially with relevance to the lungs, the stiffness of current cell culture plastics does not allow application of breathing biomechanics and does not mimic the mechanical properties of this soft, dynamic tissue (Butcher, Alliston, and Weaver 2009). Application of patient-derived AEC2 in these models will aid in elucidating how biomechanical forces related to breathing play a role in alveolar homeostasis and disease. Recently, interesting links between biomechanics and cellular function have been revealed, as illustrated by Park and colleagues (Park et al. 2020) showing that stiffness of the substrate impacts bronchial epithelial cell metabolism. Furthermore, an increase in stiffness and reduced stretch can lead to cytoskeletal reorganization which can influence integrin-mediated latent TGF-β1 activation, which in turn may contribute to disease progression in diseases such as COPD (Froese et al. 2016). However, this has not been studied in relation to alveolar epithelial cells. Organoid cultures could support studies on epithelial biology in relation to matrix stiffness, however since there is no air-liquid interface and no application of strain, a complementary approach with stretchable Lung-Chip models is preferred. To establish proof-of-principle that the primary AEC2 obtained via our isolation protocol could be cultured under cyclic stretch in the Alveolus Lung-Chip, we exposed them to similar levels of stretch as previously reported (Hassell et al. 2017) as this was well tolerated and mimics what is expected in an alveolus (Waters, Roan, and Navajas

2012; Fredberg et al. 1997). We observed that the alveolar cells exposed to stretch slightly aligned in the direction of the flow and perpendicular to the direction of the stretch already within 24 h after initiation of stretch. It is at present unclear whether this response mimics behaviour of the alveolar cells *in situ*, especially as this response varied highly between cultures/donor mixes. Although this first proof-of-principle showed the feasibility of stretch application to these primary alveolar cell cultures, derived from healthy and end stage emphysematous lung tissue, future research will focus on the impact of different stretch intensities in combination with air-liquid interface, preferably in co-culture with other cell types in the chip such as endothelial cells and/or fibroblasts. Such extensive experiments are beyond the current proof-of-principle as AEC2 cultures would need to be further upscaled. In addition, running combinations of different flow and stretch conditions on-Chip in the same experiment is still restricted due to the current level or resources needed for such a set-up using this technology.

In conclusion, we demonstrate the successful isolation of AEC2 from diseased human lung tissue which can subsequently be expanded using feeder-free organoid culture. The organoids retain expression of AEC2 markers over time and can be dissociated for further experiments. We showed the feasibility of culturing these patient-derived AEC2 in the Alveolus Lung-Chip under application of cyclic strain. This method is expected to aid future research on how forces related to breathing contribute to alveolar homeostasis and disease, which is needed in view of the important gaps in our knowledge of cellular biomechanics of the human alveolus in health and disease.

Acknowledgement

We would like to thank Emulate, especially Geraldine Hamilton and Lorna Ewart for their support in the development of the Alveolus Lung-Chip cultures. We would like to thank the LUMC Light and Electron Microscopy Facility for technical assistance during imaging of the Alveolus Lung-Chip.
This study was supported by a grant of the Lung Foundation Netherlands (grant # 6.1.14.010), The Netherlands Organization for Health Research and Development (ZonMw; grant #114021508), Translationeel Adult Stamcelonderzoek – ZonMw (TAS-ZonMW; grant #40414009816007), EU Marie Curie Global Fellowship (#748569), Stichting Proefdiervrij.

Author contributions

Conception and design: SR, AS, PK, PH, AD; Patient selection and sample preparation: SR, AS, PK, JS, AD; Analysis and interpretation: SR, AS, PH, AD; Drafting the manuscript for important intellectual content: SR, AS, PK, JS, PH, AD. All authors have read the manuscript, provided input and agree with its submission.

References

Agusti, A., and J. C. Hogg. 2019. 'Update on the Pathogenesis of Chronic Obstructive Pulmonary Disease', N Engl J Med, 381: 1248-56.

Benam, K. H., R. Villenave, C. Lucchesi, A. Varone, C. Hubeau, H. H. Lee, S. E. Alves, M. Salmon, T. C. Ferrante, J. C. Weaver, A. Bahinski, G. A. Hamilton, and D. E. Ingber. 2016. 'Small airway-on-a-chip enables analysis of human lung inflammation and drug responses *in vitro*', Nat Methods, 13: 151-7.

Butcher, D. T., T. Alliston, and V. M. Weaver. 2009. 'A tense situation: forcing tumour progression', Nat Rev Cancer, 9: 108-22.

Celli, B. R., and J. A. Wedzicha. 2019. 'Update on Clinical Aspects of Chronic Obstructive Pulmonary Disease', N Engl J Med, 381: 1257-66.

Choi, J., J. E. Park, G. Tsagkogeorga, M. Yanagita, B. K. Koo, N. Han, and J. H. Lee. 2020. 'Inflammatory Signals Induce AT2 Cell-Derived Damage-Associated Transient Progenitors that Mediate Alveolar Regeneration', Cell Stem Cell, 27: 366-82 e7.

Evans, K. V., and J. H. Lee. 2020. 'Alveolar wars: The rise of *in vitro* models to understand human lung alveolar maintenance, regeneration, and disease', Stem Cells Transl Med, 9: 867-81.

Fredberg, J. J., D. Inouye, B. Miller, M. Nathan, S. Jafari, S. H. Raboudi, J. P. Butler, and S. A. Shore. 1997. 'Airway smooth muscle, tidal stretches, and dynamically determined contractile states', Am J Respir Crit Care Med, 156: 1752-9.

Froese, A. R., C. Shimbori, P. S. Bellaye, M. Inman, S. Obex, S. Fatima, G. Jenkins, J. Gauldie, K. Ask, and M. Kolb. 2016. 'Stretch-induced Activation of Transforming Growth Factor-beta1 in Pulmonary Fibrosis', Am J Respir Crit Care Med, 194: 84-96.

Glisinski, K. M., A. J. Schlobohm, S. V. Paramore, A. Birukova, M. A. Moseley, M. W. Foster, and C. E. Barkauskas. 2020. 'Interleukin-13 disrupts type 2 pneumocyte stem cell activity', JCI Insight, 5.

Gonzalez, R. F., L. Allen, L. Gonzales, P. L. Ballard, and L. G. Dobbs. 2010. 'HTII-280, a biomarker specific to the apical plasma membrane of human lung alveolar type II cells', J Histochem Cytochem, 58: 891-901.

Hassell, B. A., G. Goyal, E. Lee, A. Sontheimer Phelps, O. Levy, C. S. Chen, and D. E. Ingber. 2017. 'Human Organ Chip Models Recapitulate Orthotopic Lung Cancer Growth, Therapeutic Responses, and Tumor Dormancy *In Vitro*', Cell Rep, 21: 508-16.

Hiemstra, P. S., T. D. Tetley, and S. M. Janes. 2019. 'Airway and alveolar epithelial cells in culture', Eur Respir J, 54.

Hogg, J. C., and W. Timens. 2009. 'The pathology of chronic obstructive pulmonary disease', Annu Rev Pathol, 4: 435-59.

Huh, D. D. 2015. 'A human breathing lung-on-a chip', Ann Am Thorac Soc, 12 Suppl 1: S42-4.

Huh, D., B. D. Matthews, A. Mammoto, M. Montoya-Zavala, H. Y. Hsin, and D. E. Ingber. 2010. 'Reconstituting organ-level lung functions on a chip', Science, 328: 1662-8.

Jacob, A., M. Morley, F. Hawkins, K. B. McCauley, J. C. Jean, H. Heins, C. L. Na, T. E. Weaver, M. Vedaie, K. Hurley, A. Hinds, S. J. Russo, S. Kook, W. Zacharias, M. Ochs, K. Traber, L. J. Quinton, A. Crane, B. R. Davis, F. V. White, J. Wambach, J. A. Whitsett, F. S. Cole, E. E. Morrisey, S. H. Guttentag, M. F. Beers, and D. N. Kotton. 2017. 'Differentiation of Human Pluripotent Stem Cells into Functional Lung Alveolar Epithelial Cells', Cell Stem Cell, 21: 472-88 e10.

Katsura, H., V. Sontake, A. Tata, Y. Kobayashi, C. E. Edwards, B. E. Heaton, A. Konkimalla, T. Asakura, Y. Mikami, E. J. Fritch, P. J. Lee, N. S. Heaton, R. C. Boucher, S. H. Randell, R. S. Baric, and P. R. Tata. 2020. 'Human Lung Stem Cell-Based Alveolospheres Provide Insights into SARS-CoV-2-Mediated Interferon Responses and Pneumocyte Dysfunction', Cell Stem Cell.

Khakban, A., D. D. Sin, J. M. FitzGerald, B. M. McManus, R. Ng, Z. Hollander, and M. Sadatsafavi. 2017. 'The Projected Epidemic of Chronic Obstructive Pulmonary Disease Hospitalizations over the Next 15 Years. A Population-based Perspective', Am J Respir Crit Care Med, 195: 287-91.

Kobayashi, Y., A. Tata, A. Konkimalla, H. Katsura, R. F. Lee, J. Ou, N. E. Banovich, J. A. Kropski, and P. R. Tata. 2020. 'Persistence of a regeneration-associated, transitional alveolar epithelial cell state in pulmonary fibrosis', Nat Cell Biol, 22: 934-46.

Lamers, M. M., J. van der Vaart, K. Knoops, S. Riesebosch, T. I. Breugem, A. Z. Mykytyn, J. Beumer, D. Schipper, K. Bezstarosti, C. D. Koopman, N. Groen, R. B. G. Ravelli, H. Q. Duimel, J. A. A. Demmers, Gmgm Verjans, M. P. G. Koopmans, M. J. Muraro, P. J. Peters, H. Clevers, and B. L. Haagmans. 2021. 'An organoid-derived bronchioalveolar model for SARS-CoV-2 infection of human alveolar type II-like cells', EMBO J, 40: e105912.

Mao, P., S. Wu, J. Li, W. Fu, W. He, X. Liu, A. S. Slutsky, H. Zhang, and Y. Li. 2015. 'Human alveolar epithelial type II cells in primary culture', Physiol Rep, 3.

Miravitlles, M., C. Vogelmeier, N. Roche, D. Halpin, J. Cardoso, A. G. Chuchalin, H. Kankaanranta, T. Sandstrom, P. Sliwinski, J. Zatloukal, and F. Blasi. 2016. 'A review of national guidelines for management of COPD in Europe', Eur Respir J, 47: 625-37.

Nabhan, A. N., D. G. Brownfield, P. B. Harbury, M. A. Krasnow, and T. J. Desai. 2018. 'Single-cell Wnt signaling niches maintain stemness of alveolar type 2 cells', Science, 359: 1118-23.

Park, J. S., C. J. Burckhardt, R. Lazcano, L. M. Solis, T. Isogai, L. Li, C. S. Chen, B. Gao, J. D. Minna, R. Bachoo, R. J. DeBerardinis, and G. Danuser. 2020. 'Mechanical regulation of glycolysis via cytoskeleton architecture', Nature, 578: 621-26.

Sachs, N., A. Papaspyropoulos, D. D. Zomer-van Ommen, I. Heo, L. Bottinger, D. Klay, F. Weeber, G. Huelsz-Prince, N. Iakobachvili, G. D. Amatngalim, J. de Ligt, A. van Hoeck, N. Proost, M. C. Viveen, A. Lyubimova, L. Teeven, S. Derakhshan, J. Korving, H. Begthel, J. F. Dekkers, K. Kumawat, E. Ramos, M. F. van Oosterhout, G. J. Offerhaus, D. J. Wiener, E. P. Olimpio, K. K. Dijkstra, E. F. Smit, M. van der Linden, S. Jaksani, M. van de Ven, J. Jonkers, A. C. Rios, E. E. Voest, C. H. van Moorsel, C. K. van der Ent, E. Cuppen, A. van Oudenaarden, F. E. Coenjaerts, L. Meyaard, L. J. Bont, P. J. Peters, S. J. Tans, J. S. van Zon, S. F. Boj, R. G. Vries, J. M. Beekman, and H. Clevers. 2019. 'Long-term expanding human airway organoids for disease modeling', EMBO J, 38.

Salahudeen, A. A., S. S. Choi, A. Rustagi, J. Zhu, V. van Unen, O. Sm de la, R. A. Flynn, M. Margalef-Catala, A. J. M. Santos, J. Ju, A. Batish, T. Usui, G. X. Y. Zheng, C. E. Edwards, L. E. Wagar, V. Luca, B. Anchang, M. Nagendran, K. Nguyen, D. J. Hart, J. M. Terry, P. Belgrader, S. B. Ziraldo, T. S. Mikkelsen, P. B. Harbury, J. S. Glenn, K. C. Garcia, M. M. Davis, R. S. Baric, C. Sabatti, M. R. Amieva, C. A. Blish, T. J. Desai, and C. J. Kuo. 2020. 'Progenitor identification and SARS-CoV-2 infection in human distal lung organoids', Nature.

Uhl, E. W., and N. J. Warner. 2015. 'Mouse Models as Predictors of Human Responses: Evolutionary Medicine', Curr Pathobiol Rep, 3: 219-23.

Waters, C. M., E. Roan, and D. Navajas. 2012. 'Mechanobiology in lung epithelial cells: measurements, perturbations, and responses', Compr Physiol, 2: 1-29.

Witherden, I. R., and T. D. Tetley. 2001. 'Isolation and Culture of Human Alveolar Type II Pneumocytes', Methods Mol Med, 56: 137-46.

World Health Organization. 2018. 'The top 10 causes of death'. http://www.who.int/mediacentre/factsheets/fs310/en/

Zacharias, W. J., D. B. Frank, J. A. Zepp, M. P. Morley, F. A. Alkhaleel, J. Kong, S. Zhou, E. Cantu, and E. E. Morrisey. 2018. 'Regeneration of the lung alveolus by an evolutionarily conserved epithelial progenitor', Nature, 555: 251-55.

Zamprogno, P., S. Wuthrich, S. Achenbach, G. Thoma, J. D. Stucki, N. Hobi, N. Schneider-Daum, C. M. Lehr, H. Huwer, T. Geiser, R. A. Schmid, and O. T. Guenat. 2021. 'Second-generation lung-on-a-chip with an array of stretchable alveoli made with a biological membrane', Commun Biol, 4: 168.

Zhao, L., M. Yee, and M. A. O'Reilly. 2013. 'Transdifferentiation of alveolar epithelial type II to type I cells is controlled by opposing TGF-beta and BMP signaling', Am J Physiol Lung Cell Mol Physiol, 305: L409-18